

Levels in Zr^{90} : Theoretical

B. F. BAYMAN, A. S. REINER,* AND R. K. SHELIN†
Institute for Theoretical Physics, University of Copenhagen, Copenhagen, Denmark

(Received December 4, 1958)

An attempt is made to describe the seven levels of Zr^{90} below 3.6 Mev in terms of the proton configurations $(2p_{1/2})^2$, $(2p_{1/2} 1g_{9/2})$, and $(1g_{9/2})^2$. The level positions and the compositions of the two $0+$ states are determined for Gaussian and Yukawa forces of various ranges and exchange characters. The experimental data are well reproduced for a reasonable choice of the force parameters, the best fit being obtained with a Serber exchange mixture and a range of about 1.5 fermis. The experimental values of the half-lives of the excited states can also be reconciled with these simple configurational assignments. The most serious discrepancy is in the half-life of the first excited ($0+$) state, which we calculate to be 1.35×10^{-8} sec, as compared to the observed value of $(6.0 \pm 1.5) \times 10^{-8}$ sec. The remaining discrepancies in the energies and half-lives are in the direction of the effects produced by a slight deformation of the Sr^{88} core.

1. INTRODUCTION

FORD¹ has suggested that the low-lying levels of ${}_{40}Zr^{90}$ can be understood in terms of configurations obtained by distributing two protons in the $2p_{1/2}$ and $1g_{9/2}$ shells. It is certainly reasonable to deal with proton configurations alone, since the 50 neutrons form a very stable closed shell whose excitations are unlikely to affect levels below about 5 Mev. Moreover, although the single-particle proton levels in this vicinity are not known with certainty, a scheme such as that shown in Fig. 1 seems reasonable.² We need only note that the $2p_{1/2}$ - $1g_{9/2}$ spacing is probably a good deal smaller than the $1f_{5/2}$ - $2p_{1/2}$ or $2p_{3/2}$ - $2p_{1/2}$ spacings. Hence one might expect that levels involving excitations of the $1f_{5/2}$ and $2p_{3/2}$ closed shells lie higher in the Zr^{90} spectrum than those arising from the $(2p_{1/2})^2$, $(2p_{1/2} 1g_{9/2})$, and $(1g_{9/2})^2$ configurations. In addition, Ford was able to show qualitatively that the positions of the levels known at that time ($0+$, $0+$, $2+$, $5-$) could easily be understood in terms of this picture.

Since then, much more data on the excited levels of Zr^{90} have become available. In particular, $4+$, $6+$, and $8+$ levels have been found, and one is tempted to regard these as the remaining levels of the $(1g_{9/2})^2$ configuration. Accordingly, we have thought it worth while to do a detailed spectroscopic calculation based on the levels arising from these lowest three configurations, using finite-range, spin-dependent, central forces. An analysis of the observed transition probabilities provides a further check on our configurational assignments.

* C.E.R.N. Fellow 1957, on leave of absence from The Institute for Theoretical Physics, University of Amsterdam, Amsterdam, Holland. Present address: The Weizmann Institute of Science, Rehovoth, Israel.

† Member of the Institute of Theoretical Physics, 1955-1958: Present address: Chemistry Department, Florida State University, Tallahassee, Florida.

¹ K. W. Ford, Phys. Rev. **98**, 1516 (1955).

² See, for example, the spectrum of Y^{89} given by Strominger, Hollander, and Seaborg, Revs. Modern Phys. **30**, 585 (1958).

2. EXPERIMENTAL FACTS RELATING TO THE Zr^{90} SPECTRUM

The experimentally determined level scheme is shown in Fig. 9 of the preceding paper,³ where the attribution of spins and parities is discussed. It is important for our purpose to note that we have every energy level expected from the $(2p_{1/2})^2$, $(2p_{1/2} 1g_{9/2})$, and $(1g_{9/2})^2$ configurations, with the exception of the $(2p_{1/2} 1g_{9/2})_{4-}$ level.⁴ However, it is reasonable that such a level would be populated very weakly in the processes that have so far been used to excite the higher levels of Zr^{90} .

We must expect a strong interaction between the $(2p_{1/2})^2_0$ and $(1g_{9/2})^2_0$ levels, and hence the two observed $0+$ levels will be mixtures of these. We will now estimate the compositions of these mixtures from the relative populations of the observed $0+$ levels, both by β^- decay of Y^{90} and by γ decay of the Zr^{90} $2+$ level. These compositions are experimental data, independent of the positions of the levels, which can be compared to the result of a spectroscopic calculation.

Figure 2 shows the levels involved in this decay, together with the configurations that can reasonably

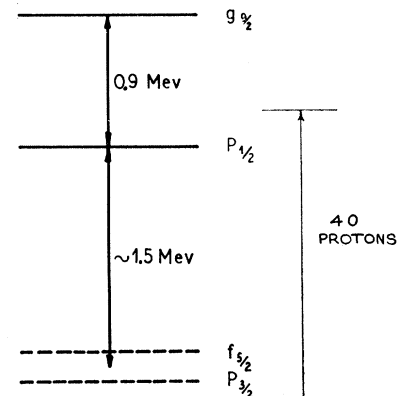
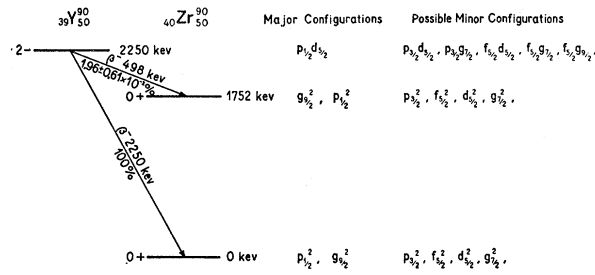


FIG. 1. Single-particle proton levels in the vicinity of $Z=40$.

³ Björnholm, Nielsen, and Shelin, preceding paper [Phys. Rev. **115**, 1613 (1959)].

⁴ The subscript outside the parentheses is the total angular momentum to which the enclosed angular momenta are vector coupled.

FIG. 2. Configurations involved in the β decay of Y^{90} .

be expected to contribute to them. The ground state of Y^{90} is $(2p_{1/2} 2d_{5/2})_{2-}$. Transitions connecting two "minor" configurations, i.e., configurations which have no particles in either the $2p_{1/2}$ or $2d_{5/2}$ orbits, should have a very small effect on the total β -decay process. The dominant contribution is from the transition $(2p_{1/2} 2d_{5/2})_{2-} \rightarrow (2p_{1/2})_{2-}^2$, while the remaining possibility, $(2p_{1/2} 2d_{5/2})_{2-} \rightarrow (2d_{5/2})_{2-}^2$, would perhaps have an effect intermediate, but still small compared to the transition between the major configurations. Hence, the comparative strengths of the β transitions to the two $0+$ levels of Zr^{90} are a measure of the relative contributions of $(2p_{1/2})_{0+}^2$ to them.

In accordance with this picture, we write the wave functions of the $0+$ ground and first excited states (hereafter referred to as $0+$ and $0'+$, respectively) as follows:

$$\begin{aligned} \psi_{0+} &= \frac{a}{(a^2+b^2)^{1/2}} \psi[(2p_{1/2})_{2-}^2] + \frac{b}{(a^2+b^2)^{1/2}} \psi[(1g_{9/2})_{2-}^2], \\ \psi_{0'+} &= \frac{-b}{(a^2+b^2)^{1/2}} \psi[(2p_{1/2})_{2-}^2] + \frac{a}{(a^2+b^2)^{1/2}} \psi[(1g_{9/2})_{2-}^2]. \end{aligned} \quad (1)$$

The ratio of the two transition probabilities is then

$$\begin{aligned} \frac{P_{Y^{90} \rightarrow Zr^{90} 0+}}{P_{Y^{90} \rightarrow Zr^{90} 0'+}} &= \frac{\left| \int \psi^* [(2d_{5/2}, 2p_{1/2})_{2-}] \theta_{\beta} \psi_{0+} d\tau \right|^2}{\left| \int \psi^* [(2d_{5/2}, 2p_{1/2})_{2-}] \theta_{\beta} \psi_{0'+} d\tau \right|^2} \\ &= \frac{a^2 f_1(2250)}{b^2 f_1(498)}, \end{aligned} \quad (2)$$

where θ_{β} is the β -decay operator, and the f_1 's are Fermi functions for a unique first-forbidden transition.

Yuasa *et al.*⁵ and Greenberg and Deutsch⁶ have determined the number of internal conversion electrons and the number of pairs resulting from the population of the $0+$ level in Zr^{90} as $(1.6 \pm 0.6) \times 10^{-4}$ and $(0.36 \pm 0.09) \times 10^{-4}$ per Y^{90} disintegration. These values imply that the $0+$ level is populated with a probability

⁵ Yuasa, Laberrigue-Frolow, and Feuvrais, *Compt. rend.* **242**, 2129 (1956).

⁶ J. Greenberg and M. Deutsch, *Phys. Rev.* **98**, 1517 (1955).

$(1.96 \pm 0.61) \times 10^{-4}$ times that of the $0+$ ground state. The rather large uncertainty here is due to that involved in the determination of the internal conversion probability. The theoretical value of $\epsilon_{KLM}/\text{Pairs} = 3$ can be inferred from the calculations of Thomas.⁷ Taken together with the experimental pair probability determined by Greenberg and Deutsch, this leads to a value of $(1.44 \pm 0.36) \times 10^{-4}$ for the relative population of the $0+$ level. These populations imply that the ratio in (2) equals $(5.1_{-1.2}^{+2.3}) \times 10^3$ and $(6.9_{-1.4}^{+2.8}) \times 10^3$, respectively.

Using the tables of Feenberg and Trigg,⁸ and making the corrections appropriate to unique first-forbidden transitions,⁹ we calculate

$$f_1(2250)/f_1(498) = 4.05 \times 10^{-3}.$$

The ratio a^2/b^2 , as calculated from (2) is $1.26_{-0.30}^{+0.57}$ or $1.70_{-0.33}^{+0.58}$, depending on whether the experimental or theoretical internal conversion frequency is used. This corresponds to $a^2 = (56_{-7}^{+9})\%$, $b^2 = (44_{+7}^{-9})\%$ in the former case, and $a^2 = (63_{-5}^{+7})\%$, $b^2 = (37_{+5}^{-7})\%$ in the latter.

An independent estimate of the compositions of the two $0+$ levels is afforded by the γ decay of the $2+$ level. Here we have

$$\begin{aligned} \frac{P_{Zr^{90} 2+ \rightarrow Zr^{90} 0+}}{P_{Zr^{90} 2+ \rightarrow Zr^{90} 0'+}} &= \frac{\left| \int \psi^* [(1g_{9/2})_{2+}^2] M_{E2} \psi_{0+} d\tau \right|^2}{\left| \int \psi^* [(1g_{9/2})_{2+}^2] M_{E2} \psi_{0'+} d\tau \right|^2} \\ &\times \left(\frac{2182-0}{2182-1752} \right)^5 \\ &= (b^2/a^2) \times 3400. \end{aligned} \quad (3)$$

Although the very weak 430-keV γ transition between the $2+$ and $0'+$ levels is seen, there is considerable uncertainty regarding the observed intensity. Therefore we estimate this by subtracting the probability of the $0'+ \rightarrow 0+$ transition from that of the $2+ \rightarrow 0+$ transition. The former probability is calculated from the well-determined 1734-keV conversion (intensity 5.5×10^{-5} per disintegration) and the theoretical pair probability of Thomas.⁷ The latter probability is measured directly.

The validity of this procedure depends on the assumption that the $0'+$ level is populated entirely by transitions from the $2+$ level. Certainly we can treat as insignificant contributions to the $0'+$ level from the levels at 3081 keV ($4+$), 3452 keV ($6+$), and 3595 keV ($8+$). The 5-level should populate the $0'+$ level with a frequency of about $(563/2315)^{11} \times 0.84 = 1.5 \times 10^{-7}$ transitions per disintegration. This is also insignificant

⁷ P. Thomas, *Phys. Rev.* **58**, 714 (1940).

⁸ E. Feenberg and G. Trigg, *Revs. Modern Phys.* **22**, 399 (1950).

⁹ J. Davidson, *Phys. Rev.* **82**, 48 (1951).

in comparison with the population from the $2+$ level. We calculate $(b^2/a^2)3400 = (1.4 \pm 0.2) \times 10^{-1} / (7.34 \pm 0.7) \times 10^{-5}$ leading to values of b^2 and a^2 of $(36_{-5}^{+6})\%$ and $(64_{-6}^{+5})\%$, respectively. This excellent agreement with the estimate based on the β decay of Y^{90} gives us confidence in the validity of our picture. The two estimates are independent, not only with respect to the experimental quantities involved, but also in that one measures the $(2p_{1/2})^2$ contribution to each $0+$ level, the other the $(1g_{9/2})^2$ contribution.

Our conclusion is that the composition of the Zr^{90} ground state is $(63 \pm 5)\%$ $(2p_{1/2})^2$ and $(37 \pm 5)\%$ $(1g_{9/2})^2$. These percentages are interchanged for the 1752-kev $0+$ level.

3. SPECTROSCOPIC CALCULATION

As stated in the Introduction, we calculate the levels of Zr^{90} using a model of two protons in the $(2p_{1/2})^2$, $(1g_{9/2})^2$, and $(2p_{1/2} 1g_{9/2})$ configurations. We need, however, further assumptions about the single-particle radial wave functions and the two-particle interaction.

We follow here the usual practice of taking the single-particle wave functions to be those of a particle moving in a spherically symmetrical harmonic oscillator field,

$$H_{s.p.} = p^2/2m + (m\omega^2/2)r^2. \quad (4)$$

We can estimate ω by identifying the expectation value of r^2 , averaged over the 90 nucleons in Zr^{90} , with $\frac{3}{5}R^2$, where R is the nuclear radius. Thus

$$\begin{aligned} \langle (N + \frac{3}{2}) \rangle_n \hbar\omega/2 &= \frac{1}{2}m\omega^2 \langle r^2 \rangle = \frac{1}{2}m\omega^2 (\frac{3}{5}R^2) \\ &= \frac{1}{2}m\omega^2 (\frac{3}{5}) (1.3 \times 90^{\frac{1}{3}} \times 10^{-13} \text{ cm})^2, \end{aligned} \quad (5)$$

$$\hbar\omega \sim 8 \text{ Mev}, \quad m\omega/\hbar \equiv \alpha^2 \sim 1.9 \times 10^{25} \text{ cm}^{-2}.$$

The radial functions we need are

$$u_{1g}(r) = \pi^{-\frac{1}{2}} \alpha^{\frac{3}{2}} \frac{8}{(9!!)^{\frac{1}{2}}} (\alpha r)^4 \exp[-\frac{1}{2}(\alpha r)^2], \quad (6)$$

$$u_{2p}(r) = \pi^{-\frac{1}{2}} \alpha^{\frac{3}{2}} \frac{4}{(5!!)^{\frac{1}{2}}} (\alpha r) [\frac{5}{2} - (\alpha r)^2] \exp[-\frac{1}{2}(\alpha r)^2],$$

where $(2n+1)!! \equiv 1 \times 3 \times 5 \times \dots \times (2n+1)$.

The two-particle interactions we investigate are of the form

$$V_{12} = \{-0.6Q^S + \tau Q^T\} V(r_{12}) + e^2/r_{12}, \quad (7)$$

with

$$V(r_{12}) = V_0 \frac{e^{-(r_{12}/\rho)}}{(r_{12}/\rho)} \quad (\text{Yukawa}), \quad (8)$$

or

$$V(r_{12}) = V_0 \exp(-r_{12}^2/2\sigma^2) \quad (\text{Gauss}). \quad (9)$$

Here Q^S and Q^T are projection operators which select the singlet and triplet parts, respectively, of the

2 -proton wave functions. The Rosenfeld exchange mixture uses $\tau = \frac{1}{3}$.

The matrix elements we need can then be calculated using the expression

$$\begin{aligned} \langle j_1 j_2; J | V_{12} | j_1' j_2'; J \rangle &= -0.6 \langle (l_{1\frac{1}{2}})_{j_1} (l_{2\frac{1}{2}})_{j_2} | (l_1 l_2)_J (\frac{1}{2}\frac{1}{2})_0 \rangle_J \\ &\quad \times \langle (l_1' \frac{1}{2})_{j_1'} (l_2' \frac{1}{2})_{j_2'} | (l_1' l_2')_J (\frac{1}{2}\frac{1}{2})_0 \rangle_J \\ &\quad \times \sum_k (-1)^k F^k U(l_1 k J l_2'; l_1' l_2') (k l_1' 0 0 | l_1 0) \\ &\quad \times (k l_2' 0 0 | l_2 0) + \tau \sum_L \langle (l_{1\frac{1}{2}})_{j_1} (l_{2\frac{1}{2}})_{j_2} | (l_1 l_2)_L (\frac{1}{2}\frac{1}{2})_1 \rangle_J \\ &\quad \times \langle (l_1' \frac{1}{2})_{j_1'} (l_2' \frac{1}{2})_{j_2'} | (l_1' l_2')_L (\frac{1}{2}\frac{1}{2})_1 \rangle_J \\ &\quad \times \sum_k (-1)^k F^k U(l_1 k L l_2'; l_1' l_2') \\ &\quad \quad \quad \times (k l_1' 0 0 | l_1 0) (k l_2' 0 0 | l_2 0). \end{aligned} \quad (10)$$

The j - j to L - S transformation coefficients are given by Flowers,¹⁰ or may also be obtained from the convenient table given by Racah.¹¹ The radial integrals F^k were calculated, using the method of Talmi,¹² as linear combinations of the simpler integrals, I_l , viz.

$$F^k = \sum_l c_l^k I_l, \quad (11)$$

where

$$I_l \equiv \frac{V_0 \alpha^{2l+3}}{(2l+1)!!} \left(\frac{2}{\pi}\right)^{\frac{1}{2}} \int_0^\infty \exp[-\frac{1}{2}\alpha^2 r^2] r^{2l+2} V(r) dr. \quad (12)$$

The c_l^k for the $(1g_{9/2})^2$ and $(2p_{1/2})^2$ configurations were taken from the tabulation by Thieberger.¹³ For the $(2p_{1/2} 1g_{9/2})$ configuration and the $\langle (2p_{1/2})^2_0 | V_{12} | (1g_{9/2})^2_0 \rangle$ matrix element, we need in addition the expressions given in the Appendix. Explicit formulas for the I_l are:

Coulomb interaction:

$$I_l = \frac{938}{137} \left(\frac{2}{\pi}\right)^{\frac{1}{2}} \alpha \frac{(2l)!}{[(2l+1)!!]^2} \text{ Mev}; \quad (13)$$

Gauss interaction:

$$I_l = V_0 \left[\frac{\lambda^2}{1+\lambda^2} \right]^{l+\frac{1}{2}} \text{ Mev}, \quad \lambda = \alpha\sigma; \quad (14)$$

Yukawa interaction:

$$I_l = V_0 \left(\frac{2}{\pi}\right)^{\frac{1}{2}} \frac{e^{(\kappa^2/2)}}{\kappa} 2^l l! \text{Hh}_{2l+1}(\kappa) \text{ Mev}, \quad \kappa = (\alpha\rho)^{-1}. \quad (15)$$

To calculate a spectrum, we must choose an exchange mixture (τ), an interaction shape (Gauss or Yukawa), a range (λ or κ), and strength (V_0). The levels $(1g_{9/2})^2_{2,4,6,8}$

¹⁰ B. H. Flowers, Proc. Roy. Soc. (London) **A215**, 398 (1952).

¹¹ G. Racah, Physica **16**, 651 (1950).

¹² I. Talmi, Helv. Phys. Acta **25**, 185 (1952).

¹³ R. Thieberger, Nuclear Phys. **2**, 533 (1956-57).

$$V(r) = \frac{e^2}{r} + \left\{ -0.6 Q_8^5 + \tau Q_7^1 \right\} V_0 e^{-\frac{\alpha^2 r^2}{2\lambda^2}}$$

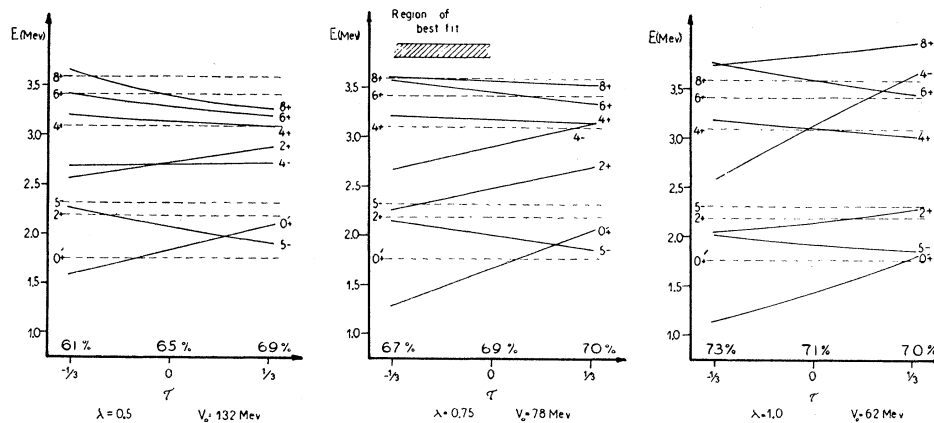


FIG. 3. Experimental and calculated spectra. Solid lines: calculated levels as functions of triplet strength τ . Dashed lines: experimental levels (no 4-level has been seen). Numbers above τ axes: calculated $(2p_{1/2})^2_0$ contributions to ground state, the experimental value is $(63 \pm 5)\%$.

are simply given by $\langle (1g_{9/2})^2_J | V_{12} | (1g_{9/2})^2_J \rangle$, the levels $(2p_{1/2} 1g_{9/2})_{4,5}$ by $\langle (2p_{1/2} 1g_{9/2})_J | V_{12} | (2p_{1/2} 1g_{9/2})_J \rangle - 0.91$. For the two $0+$ levels, we must diagonalize the matrix

$$\begin{bmatrix} \langle (1g_{9/2})^2_0 | V_{12} | (1g_{9/2})^2_0 \rangle & \langle (2p_{1/2})^2_0 | V_{12} | (1g_{9/2})^2_0 \rangle \\ \langle (2p_{1/2})^2_0 | V_{12} | (1g_{9/2})^2_0 \rangle & \langle (2p_{1/2})^2_0 | V_{12} | (2p_{1/2})^2_0 \rangle - 1.82 \end{bmatrix}, \quad (16)$$

where we have taken the single-particle $2p_{1/2}$ - $1g_{9/2}$ spacing to be 0.91 Mev (see the discussion in Sec. 1). In this way, we have calculated spectra corresponding to $\tau = -\frac{2}{3}, -\frac{1}{3}, 0, \frac{1}{3}, \frac{2}{3}$, the values of λ and κ shown in Table I, and for a range of strengths V_0 for each choice of τ and λ or κ . Figure 3 shows some of the spectra obtained with the Gaussian interaction. The results for the Yukawa interaction are very similar, except that the fit with experiment is slightly poorer. We have also indicated in Fig. 3 the calculated compositions of the two $0+$ states.

4. EFFECT OF MODIFICATIONS OF THE FORCE

We will now consider the way the positions of the calculated levels depend upon the various assumptions described in the previous section. To this end we note that the expectation values of our interactions in all the states except the $0+$ and $0'+$ are of the form [see Eqs. (10), (11), and (12)]

TABLE I. Ranges used in the calculation.

Gauss: $\exp[-(r^2/2\sigma^2)]$		Yukawa: $(\rho/r)^{-1} \exp[-r/\rho]$	
λ	σ (cm)	κ	ρ (cm)
0.5	1.15×10^{-13}	0.3	7.5×10^{-13}
0.75	1.72×10^{-13}	0.9	2.5×10^{-13}
1.0	2.3×10^{-13}	1.5	1.5×10^{-13}

$$\begin{aligned} E_J &= \sum_l \left[-0.6a_l [S, (1g_{9/2})^2_J] + \tau a_l [T, (1g_{9/2})^2_J] \right] I_l, \\ &= V_0 \sum_l \left[-0.6a_l [S, (1g_{9/2})^2_J] + \tau a_l [T, (1g_{9/2})^2_J] \right] \\ &\quad \times \frac{\alpha^{2l+3}}{(2l+1)!!} \left(\frac{2}{\pi} \right)^{\frac{1}{2}} \int_0^\infty \exp(-\frac{1}{2}\alpha^2 r^2) V(r) r^{2l+2} dr \\ &= V_0 \left[-0.6 \int_0^\infty V(r) dr \left\{ \sum_l a_l [S, (1g_{9/2})^2_J] \right. \right. \\ &\quad \times \frac{\alpha^{2l+3}}{(2l+1)!!} \left(\frac{2}{\pi} \right)^{\frac{1}{2}} \exp(-\frac{1}{2}\alpha^2 r^2) r^{2l+2} \left. \left. \right\} \right. \\ &\quad \left. + \tau \int_0^\infty V(r) dr \left\{ \sum_l a_l [T, (1g_{9/2})^2_J] \right. \right. \\ &\quad \left. \left. \times \frac{\alpha^{2l+3}}{(2l+1)!!} \left(\frac{2}{\pi} \right)^{\frac{1}{2}} \exp(-\frac{1}{2}\alpha^2 r^2) r^{2l+2} \right. \right. \left. \left. \right\} \right]. \quad (17) \end{aligned}$$

We can therefore identify the functions

$$\begin{aligned} P_S^J(r) &\equiv \left(\frac{2}{\pi} \right)^{\frac{1}{2}} \sum_l a_l [S, (1g_{9/2})^2_J] \\ &\quad \times \frac{\alpha^{2l+3}}{(2l+1)!!} \exp(-\frac{1}{2}\alpha^2 r^2) r^{2l+2}, \\ P_T^J(r) &\equiv \left(\frac{2}{\pi} \right)^{\frac{1}{2}} \sum_l a_l [T, (1g_{9/2})^2_J] \\ &\quad \times \frac{\alpha^{2l+3}}{(2l+1)!!} \exp(-\frac{1}{2}\alpha^2 r^2) r^{2l+2}, \quad (18) \end{aligned}$$

with the probability distributions of relative distance in the singlet and triplet parts of the two-particle state ψ_J . Moreover, the symmetry¹⁴ between position and linear momentum in the harmonic oscillator Hamiltonian (4) implies that these functions also give the probability distribution of relative momentum, provided that we interpret α as $(m\omega\hbar)^{-\frac{1}{2}}$. They are plotted in Figs. 4 and 5. Using the estimate (5) of $\hbar\omega=8$ Mev, we see that our wave functions contain appreciable components with relative energies up to 100 Mev.

The probability distributions for the two $0+$ states involve an assumption about their compositions in terms of $(2p_{1/2})^2_0$ and $(1g_{9/2})^2_0$ states. Figures 4 and 5 use the mixtures

$$\psi_{0+} = 0.8\psi[(2p_{1/2})^2_0] - 0.6\psi[(1g_{9/2})^2_0] \quad (\text{ground state}), \quad (19a)$$

$$\psi_{0'+} = 0.6\psi[(2p_{1/2})^2_0] + 0.8\psi[(1g_{9/2})^2_0] \quad (\text{first excited state}). \quad (19b)$$

Compositions roughly equal to these were obtained for any of the force parameters we investigated. Here we have

$$\begin{aligned} P_{S^0}(r) &= \left(\frac{2}{\pi}\right)^{\frac{1}{2}} \sum_l [0.64a_l[S; (2p_{1/2})^2_0] \\ &\quad + 0.36a_l[S; (1g_{9/2})^2_0] \\ &\quad - 0.96a_l[S; (2p_{1/2})^2_0 - (1g_{9/2})^2_0]] \\ &\quad \times \frac{\alpha^{2l+3}}{(2l+1)!!} \exp(-\frac{1}{2}\alpha^2 r^2) r^{2l+2} \\ P_{S^{0'}}(r) &= \left(\frac{2}{\pi}\right)^{\frac{1}{2}} \sum_l [0.36a_l[S; (2p_{1/2})^2_0] \\ &\quad + 0.64a_l[S; (1g_{9/2})^2_0] \\ &\quad + 0.96a_l[S; (2p_{1/2})^2_0 - (1g_{9/2})^2_0]] \\ &\quad \times \frac{\alpha^{2l+3}}{(2l+1)!!} \exp(-\frac{1}{2}\alpha^2 r^2) r^{2l+2} \quad (18') \end{aligned}$$

with corresponding expressions for the triplet components.

We have also plotted in Figs. 4 and 5 the radial dependence of the three Gauss potential we have used. It is seen that, in each case, the two protons spend only a small fraction of their time within the range of the assumed forces, and that the strength of interaction in any state J depends only on the behavior of $P_{S^J}(r)$ and $P_{T^J}(r)$ for small values of r . Similar remarks apply to the three Yukawa potentials.

These curves enable us to understand the response of the energy levels to changes in the force parameters. From Fig. 5 we see that the two protons in the triplet parts of the $0'+$ and $2+$ levels spend more time within

¹⁴ We are indebted to Mr. D. Bès for this remark.

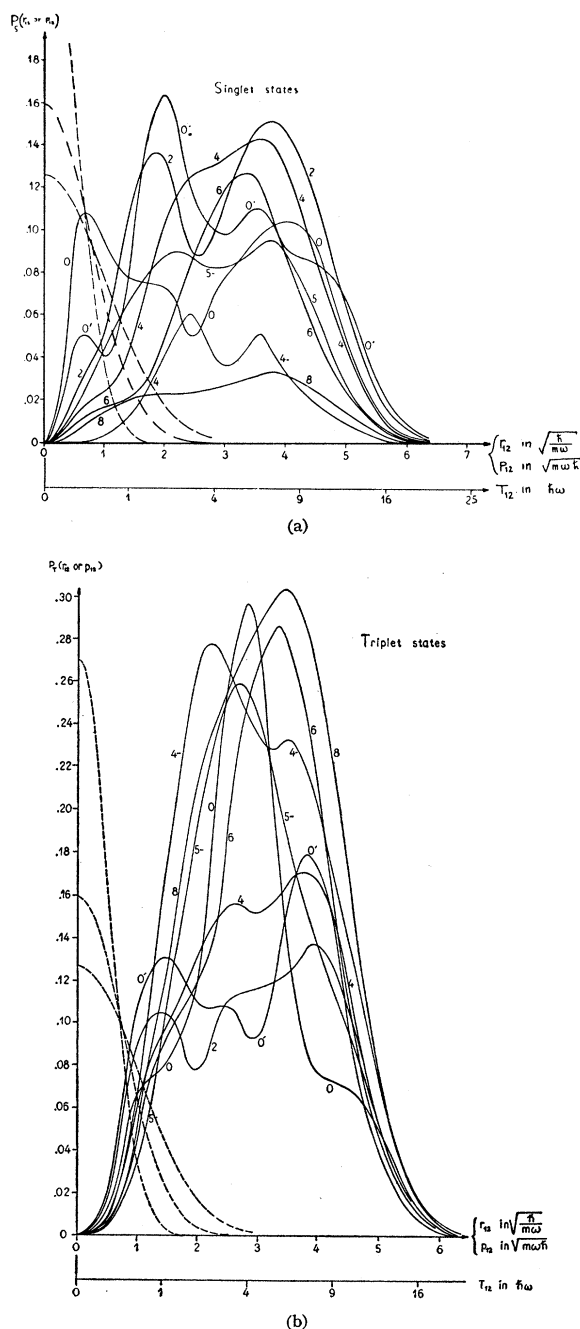


FIG. 4. Solid lines: probability distributions of relative distance and momentum implied by the assumed configurations and harmonic oscillator radial functions. Dashed lines: the three Gaussian interactions used in the calculation.

the range of a short-range force than they do in the triplet part of the lowest $0+$ level. We must therefore expect the $0'+$ and $2+$ states to be more responsive than the lowest $0+$ level to changes in the triplet force strength. Since the lowest $0+$ level is kept fixed at 0 Mev in Fig. 3, this causes the $0'+$ and $2+$ levels to rise as the triplet force becomes more repulsive, and so

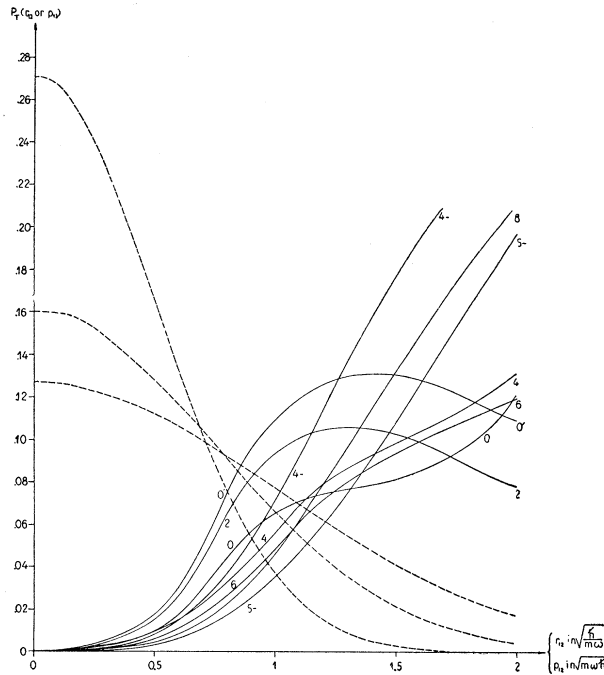


FIG. 5. The low (r_{12}, p_{12}) region of Fig. 4(b).

the corresponding curves in Fig. 3 should have positive slopes. On the other hand, the two protons in the triplet parts of the $5-$, $4+$, $6+$, and $8+$ levels spend less time close together than they do in the lowest $0+$ level, so they should be less responsive to changes in the triplet force strength, which means they should have negative slopes in Fig. 3. Both these conclusions are in accord with the actual movement of the levels. Moreover, as the range of the force increases, and the values of $P_T^J(r)$ for larger r become important, we see that the sensitivity of the ground state to changes in the triplet forces decreases with respect to that of the other levels. This leads us to expect the slopes of the curves in Fig. 6 to become more positive as we increase the force range. This should be especially true for the $4-$ and $8+$ levels, since $P_T^4(r)$ and $P_T^8(r)$ increase rapidly in the region of r available to the Gauss interaction of longest range. This feature is also exhibited by Fig. 3.

We can also discuss the movement of the calculated levels in Fig. 3 for varying force range and fixed exchange mixture. For $\tau=0$, the principal effect of increasing the range is to spread the $J=2+$, $4+$, $6+$, $8+$ levels and to diminish the $(0+)-(2+)$ spacing. We see here the transition from a level scheme of the characteristic short-range "seniority" type to one of the long-range "rotational" type.

In the "region of best fit" of Fig. 3, the remaining disagreement is greatest for the $2+$, $5-$, and $0'+$ levels. It is perhaps suggestive that collective effects would depress our calculated $2+$ level, and so improve the fit with experiment.

The calculations with a Yukawa radial dependence give essentially the same spectra and dependence on range and exchange mixture. Therefore we do not give here the actual numerical results, but only remark that we obtained best agreement with the observed levels using $\kappa=0.9$ and $V_0=42$ Mev. Elliott and Flowers¹⁵ used $\kappa=0.87$ for their calculation of levels in the nuclei around O¹⁶, and also found that $V_0\sim 40$ Mev gave best agreement with observed levels.

5. THE $(0'+)-(0+)$ LIFETIMES

Zr⁹⁰ is one of the very few nuclei with a first-excited $0'+$ state. This state (which we have designated $0'+$) can only decay by electron (or pair) emission. The transition probability for such a (monopole) transition can be written

$$W_{E0^{(e)}} = B(Z)F(Z, E, R) |M|^2. \quad (20)$$

Here $B(Z)F(Z, E, R)$ is proportional to the square of the electronic transition matrix element, of which $F(Z, E, R)$ is a factor common to all models chosen to represent the nuclear charge density. $B(Z)$ contains the specific properties of these models, and has been given elsewhere.¹⁶ $|M|^2$ is the absolute square of the nuclear transition matrix element of the monopole operator, which is defined as

$$M = \sum_{\text{protons}} r_i^2 [1 - \sigma(r_i^2/R) + \dots]. \quad (21)$$

For all but the heaviest elements, only the first term is of importance.

The wave functions of the two $0+$ states are given by (1), and permit a calculation of M once the parameters a , b are known. One easily finds¹⁷

$$\begin{aligned} M &= \frac{ab}{a^2+b^2} [\langle (1g_{9/2})^2_0 | r_1^2 + r_2^2 | (1g_{9/2})^2_0 \rangle \\ &\quad - \langle (2p_{1/2})^2_0 | r_1^2 + r_2^2 | (2p_{1/2})^2_0 \rangle] \\ &= \frac{2ab}{a^2+b^2} [\langle r^2 \rangle_{1g_{9/2}} - \langle r^2 \rangle_{2p_{1/2}}]. \end{aligned} \quad (22)$$

Equation (22) displays clearly the mechanism of the transition as a radial oscillation of charge between two "orbits." Using harmonic oscillator radial functions we have

$$[\langle r^2 \rangle_{1g_{9/2}} - \langle r^2 \rangle_{2p_{1/2}}] = \left(\frac{11}{2} - \frac{9}{2} \right) \frac{\hbar}{m\omega} = \rho R^2, \quad (23)$$

where

$$\rho = \frac{1}{\langle N + \frac{3}{2} \rangle_{Av}} \frac{3}{5} = 0.146, \quad (24)$$

according to (5). The ratio $2ab/(a^2+b^2)$ is rather

¹⁵ J. P. Elliott and B. H. Flowers, Proc. Roy. Soc. (London) **A229**, 536 (1955).

¹⁶ A. S. Reiner, Physica **23**, 33 (1957).

¹⁷ We are indebted to Dr. B. R. Mottelson for suggesting this method.

insensitive to a and b , providing neither is too small. Using the experimental values for a and b (see Sec. 2) and the values of $B(Z)$ and $F(Z, W, R)$ (the latter for K -conversion) appropriate to the transition, one finds $\tau_{1/2} = 1.80 \times 10^{-8}$ sec. The K/L ratio is about 9.5, with negligible M -conversion. The value $\epsilon_{KLM}/\text{Pairs} = 3$ calculated by Thomas then leads to a total half-life of the $0+$ level of approximately 1.35×10^{-8} sec. This must be compared with the empirical value of $(6.0 \pm 1.5) \times 10^{-8}$ sec. Thus, the calculated matrix element is too large by about a factor two.

We next consider the extent to which the above calculation depends on the use of harmonic oscillator radial functions. To this end we have calculated ρ of (23) using various central potentials, each of which implies different radial wave functions. We summarize here the results.

- (a) Infinite potential well: $\rho = 0.18$.
- (b) Finite well with depth $D = -40$ Mev: $\rho = 0.18$.
- (c) Finite well with spin-orbit force of strength ξ .

D and ξ were adapted to the binding energy of the $2p_{1/2}$ nucleon and the observed single-particle splitting $1g_{9/2} - 2p_{1/2}$. This yields $D = -38.4$ Mev, $\xi = 0.62$ Mev, and $\rho = 0.17$.

(d) Infinite potential well, but all possible admixtures to $0+$ and $0'+$ taken into account using a contact interaction (strength 1.2×10^{-36} Mev cm^3) in first order perturbation theory: $\rho = 0.28$.

All models (a)–(d) only worsen the agreement between theory and experiment, which seems to indicate that the remaining discrepancy is not associated with our special choice of radial wave functions. We have here the most serious failure of our simple configurational picture. We are investigating the possibility of the influence on this transition of center-of-mass effects.

6. OTHER LIFETIMES

We now consider whether the other known transitions between the levels of Zr^{90} can be reconciled with our description of these levels in terms of the configurations $(1g_{9/2})^2$, $(2p_{1/2})^2$, $(2p_{1/2} 1g_{9/2})$.

The probabilities per unit time of an electric 2^L -pole transition of energy $\hbar\omega$ is given by¹⁸

$$T^{(EL)} = \frac{4.4(L+1)}{[(2L+1)!!]^2 L(L+3)} \left(\frac{3}{L+3} \right)^2 \times \left(\frac{\hbar\omega}{197 \text{ Mev}} \right)^{2L+1} R^{2L} S \times 10^{21} \text{ sec}^{-1}, \quad (25)$$

¹⁸ S. Moszkowski, in *Beta- and Gamma-Ray Spectroscopy*, edited by K. Siegbahn (North-Holland Publishing Company, Amsterdam, 1955), p. 373.

where R is the nuclear radius in fermis (1 fermi $\equiv 10^{-13}$ cm). The statistical factor S is defined by

$$S = \frac{4\pi}{2J_i+1} \sum_{M_i} \sum_{M_f} \sum_M \left| \int \Theta^*(J_f, M_f) Y_{M^L} \Theta(J_i, M_i) d\Omega \right|^2, \quad (26)$$

where $\Theta(J_i, M_i)$ and $\Theta(J_f, M_f)$ are the initial and final wave functions and $\int d\Omega$ implies integration over angles and summation over spins. For the transition

$$[(lj)(l'j')]_{J-\hbar\omega^{EL}} \rightarrow [(lj)(l''j'')]_{K}, \quad (27)$$

S can be calculated to be

$$S = (2L+1)(Lj'0\frac{1}{2} | j''\frac{1}{2})^2 U(Lj''Jj; j'K)k, \quad (28)$$

where $k=1, 2$, or 4 depending on whether there are 2, 3, or 4 identical orbitals participating in the transition (27). We also need S for the transition

$$[(lj)(l'j')]_{J-\hbar\omega^{EL}} \rightarrow \alpha(lj)^2_K + \beta(l'j')^2_K. \quad (29)$$

In this case we find:

$$S = 2(2L+1)(Lj'0\frac{1}{2} | j\frac{1}{2})^2 \left\{ \alpha U(LjJj; j'K) + (-1)^{J\beta} \left(\frac{2j'+1}{2j+1} \right)^{\frac{1}{2}} U(Lj'Jj'; jK) \right\}^2. \quad (30)$$

Using (25) and (28), we calculate the half-life of a $(1g_{9/2})^2_{8+} - {}_{141.5}^{E2} \rightarrow (1g_{9/2})^2_{6+}$ transition to be 9.7×10^{-7} sec. This is to be compared with the experimental half-life of $(3.0_{-1.0}^{+1.5}) \times 10^{-7}$ sec for the $8+$ level. If we interpret this enhancement as due to collective effects, we may say that the deformation of the core effectively increases the charge on each proton outside the core by a factor of about 1.8. Elliott and Flowers¹⁵ found that the effective proton charge for $E2$ transitions in O^{17} and F^{19} is 1.5, whereas the work of True and Ford¹⁹ indicates that the corresponding value for Pb^{206} is 2.15. Hence the effective charge seems to increase systematically with nuclear size. Similarly, for a 2315-keV transition between the states $(1g_{9/2} 2p_{1/2})_{5-}$ and $[0.8(2p_{1/2})^2_0 - 0.6(1g_{9/2})^2_0]$, (25) and (29) give a half-life of 3.7 sec, compared to the measured half-life of the $5-$ level of 0.83 sec. The calculated half-life is here too sensitive to the assumed nuclear radius to enable us to conclude anything about an effective proton charge for $E5$ transitions.

Furthermore, the fact that no (less than 0.02 per disintegration) $(8+) - {}_{1280}^{E3} \rightarrow (5-)$ transition competes with the $(8+) - {}_{141.5}^{E2} \rightarrow (6+)$ transition is easily understood in terms of our picture. To connect the configurations $(1g_{9/2})^2_{8+}$ and $(1g_{1/2} 2p_{1/2})_{5-}$, an $M4$ transition would be required, with a decrease in probability by a factor of about 5×10^{-5} . However, a contri-

¹⁹ W. W. True and K. W. Ford, Phys. Rev. **109**, 1675 (1958).

bution of $(1g_{9/2} 1g_{7/2})_{8+}$ to the $8+$ level would permit a 1280-keV $E3$ transition. The half-life for $(1g_{9/2} 1g_{7/2})_{8+} -_{1280} E3 \rightarrow (1g_{9/2} 2p_{1/2})_{5-}$ is given by (25) and (28) as 3.1×10^{-8} sec, as compared to 9.7×10^{-7} sec for $(1g_{9/2})^2_{8+} -_{141.5} E2 \rightarrow (1g_{9/2})^2_{6+}$. The fact that the latter transition is observed to be at least 50 times stronger than the former indicates that the contribution of $(1g_{9/2} 1g_{7/2})_{8+}$ to the observed $8+$ level is less than 1%. This is a confirmation of the extreme $j-j$ coupling model, whose breakdown would allow mixtures such as $(1g_{9/2})^2_J$ and $(1g_{9/2} 1g_{7/2})_J$.

Of course we have not ruled out the possibility of appreciable contributions to both the $8+$ and $5-$ levels of configurations such as $[(1f_{5/2})^4_J (2p_{1/2})_0^2 (1g_{9/2})^2_J]_{8+}$ or $[(1f_{5/2})^5_{5/2} (2p_{1/2})^2_0 1g_{9/2}]_{5-}$, i.e., core excitations. Since the statistical factors for such configurations are not appreciably smaller than those given by (28) and (30), we would then have to interpret the absence of an $(8+) -_{1280} E3 \rightarrow (5-)$ transition as due to accidental phase cancellations.

Turning to the $6+$ level, we must recognize that the observed $(6+) -_{1138} E1 \rightarrow (5-)$ transition contradicts our description of these levels as $(1g_{9/2})^2_{6+}$ and $(2p_{1/2} 1g_{9/2})_{5-}$. But we also observe that 2.8% of the depopulation of the $6+$ level occurs by means of the transition $(6+) -_{371.9} E2 \rightarrow (4+)$. The existence of such a competition indicates that the 1138-keV $E1$ transition is very strongly retarded. In fact, (25) and (28) yield for $(1g_{9/2})^2_{6+} -_{371.9} E2 \rightarrow (1g_{9/2})^2_{4+}$ a half-life of 2.4×10^{-9} sec, whereas a $(6+) -_{1138} E1 \rightarrow (5-)$ transition should have a half-life of about 10^{-16} sec, assuming a statistical factor of unity. Hence the observed ratio of about 40 for the two transitions indicates that the $E1$ transition is enormously retarded, and that very small admixtures of other configurations in the $6+$ and $5-$ levels would account for the observed $E1$ transition. We cannot make this argument much more quantitative because $E1$ transitions are frequently found to be hindered relative to the half-life given by (25) and (28). We can, however, conclude that the very strong hindrance we have here is due either to the almost complete absence from the $6+$ and $5-$ levels of configurations which would allow an $E1$ transition, or to phase cancellations of the type that must be invoked if we wish to explain the absence of $(8+) -_{1280} E3 \rightarrow (5-)$ in a similar way.

An analogous, but weaker, argument shows that the dominance of the $(4+) -_{900} E2 \rightarrow (2+)$ transition over the too-weak-to-be-observed $(4+) -_{766} E1 \rightarrow (5-)$ transition implies a severe retardation of the latter, and is consistent with our assumptions about the compositions of these levels. We might further expect from (25) that the transitions $(5-) -_{132.7} E3 \rightarrow (2+)$ and $(5-) -_{2315} E5 \rightarrow (0+)$ would compete on equal terms, whereas the latter is observed to be stronger by a factor of seven.

We see, therefore, that transitions which are incon-

sistent with our simple configurational assignments are all retarded compared with those that are not. As mentioned above, this does not prove the "purity" of these configurations because of the possibility that these retardations are due to interference effects. However, it seems unlikely that the phase relations of the components of the levels would always be such as to produce such large cancellations, and therefore there appears to be good reason to believe that the contributions of other configurations to the low-lying levels of Zr^{90} are not large.

7. DISCUSSION

The previous sections show that one can come quite far in understanding the positions and compositions of the low-lying levels of Zr^{90} , and the transitions between them, in terms of the lowest configurations and simple two-particle interactions. However, there remain some real discrepancies between our calculations and experiment:

- (1) The observed $E2$ and $E5$ transitions are enhanced by a factor of about 3 or 4 over our calculated values.
- (2) The observed $2+$ level is higher, and the observed $5-$ level is lower, than our calculated positions by about 200 or 300 keV.
- (3) The observed $0+ \rightarrow 0+$ monopole transition is retarded by a factor of 4 compared to our calculated transition probability.

The discrepancies in the $E2$ and $E5$ lifetimes and the $2+$ level position can be interpreted as manifestations of the deformability of the Sr^{88} core. The monopole transition may be influenced by collective motion of a different type, i.e., center-of-mass effects.

The interactions which best reproduce the experimental level spacings are of Serber exchange character, or have a weakly attractive triplet component. The best "standard deviation" for the Gaussian radial dependence is about 1.7 fermis (depth 47 MeV), with a shorter range, 1.2 fermis (depth 79 MeV), being only slightly poorer. These latter parameters are similar to those used by Redlich²⁰ in his calculation on nuclei near O^{16} (1.06 fermis, 70.8 MeV). However, the force used by True and Ford near Pb^{206} (1.3 fermis, 32.5 MeV) is considerably weaker. Our goodness of fit deteriorates rapidly if we increase the force range beyond about 2 fermis.

8. ACKNOWLEDGMENTS

We wish to express our gratitude to Dr. A. Bohr and Dr. B. R. Mottelson for many helpful discussions throughout the course of this work. The participation by one of us (R. K. S.) was made possible in part by Fulbright and Guggenheim Memorial grants.

²⁰ M. G. Redlich, Phys. Rev. **99**, 1421 (1955).

APPENDIX

The Slater integrals for the $(2p_{1/2} 1g_{9/2})$ configuration are

$$F^k(2p, 1g) \equiv \int \int u_{2p}^2(r_1) u_{1g}^2(r_2) f^k(r_1, r_2) r_1^2 r_2^2 dr_1 dr_2,$$

$$G^k(2p, 1g) \equiv \int \int u_{2p}(r_1) u_{2p}(r_2) u_{1g}(r_1) u_{1g}(r_2) \\ \times f^k(r_1, r_2) r_1^2 r_2^2 dr_1 dr_2.$$

$$F^0(2p, 1g) = (1/3840)(385I_0 + 507I_1 + 1209I_2 - 501I_3 \\ + 1899I_4 - 231I_5 - 1573I_6 + 2145I_7),$$

$$F^2(2p, 1g) = (11/768)(35I_0 + 21I_1 + 15I_2 - 231I_3 \\ + 249I_4 + 15I_5 - 299I_6 + 195I_7),$$

$$G^3(2p, 1g) = (7/3840)(385I_0 - 811I_1 + 1289I_2 - 1707I_3 \\ + 1867I_4 - 4169I_5 + 5291I_6 - 2145I_7),$$

$$G^5(2p, 1g) = (121/3840)(35I_0 - 149I_1 + 415I_2 - 1065I_3 \\ + 1865I_4 - 1855I_5 + 949I_6 - 195I_7).$$

Elastic Scattering of N^{14} by Be^9

M. L. HALBERT AND A. ZUCKER
Oak Ridge National Laboratory,* Oak Ridge, Tennessee

(Received April 20, 1959)

Nitrogen-beryllium elastic scattering was measured over an angular range from 32 to 144 deg in the center-of-mass system with an angular resolution of about one degree. The mean energy of the incident nitrogen ions was 27.3 Mev. To distinguish elastic scattering from other events, both the scattered and the recoil particles were detected in coincidence by thin CsI(Tl) scintillation counters. The elastic scattering differential cross section is 550 mb/sterad at 32 deg c.m. It decreases monotonically and more rapidly than $\csc^4(\theta/2)$ to a shallow minimum of about 5 mb/sterad at 106 deg c.m., rises slightly, and then falls to about 2.5 mb/sterad at 144 deg c.m., the largest angle measured. The data are compared to the predictions of a sharp-cutoff model for elastic scattering, but no agreement is found between this theory and the experimental results.

INTRODUCTION

ELASTIC scattering is of considerable interest in the study of nuclear reactions and can be a useful tool for constructing nuclear potential models of all degrees of sophistication. Heavy-ion elastic scattering is susceptible to some simplifications because of the classical nature of the particles. The parameter $\eta = Z_1 Z_2 e^2 / \hbar v$ indicates the degree to which a particle may be regarded as classical and is ordinarily larger than unity in heavy ion experiments.

Previously N^{14} - N^{14} elastic scattering was studied at this laboratory.¹ More recently, the elastic scattering angular distribution of C^{12} on Au^{197} was measured by Goldberg and Reynolds.² In both of these experiments it was found that the one free parameter of the semi-classical sharp-cutoff model proposed by Blair³ can be chosen so that good agreement with the data is obtained. Theoretical considerations and experiments on elastic scattering of alpha particles from heavy elements⁴ indicate that the Blair model provides a good fit if $\eta \gg 1$, and $\sigma / \sigma_{\text{Coul}} > 1/\eta$. Both heavy ion experiments cited above fulfill these requirements.

In the present measurement 27.8-Mev nitrogen-14

ions were scattered from beryllium. This corresponds to $\eta = 3.2$, a value closer to unity than was encountered in previous experiments. Furthermore, it was found that over practically the entire angular region investigated $\sigma / \sigma_{\text{Coul}} < 1/\eta$. Thus, although previous measurements of heavy-ion scattering lay in the domain of validity of the Blair model, it is not to be expected that this model will fit the results reported here.

DESIGN OF EXPERIMENT

In this experiment it was necessary to consider certain characteristics of 28-Mev nitrogen ions, the beryllium targets, and the kinematics of the scattering process in order to develop a workable design. Care had to be taken to avoid confusing nitrogen-beryllium elastic scattering with many possible similar events. These include inelastic scattering and transfer reactions⁵ from beryllium and elastic scattering from impurities.

Self-supporting beryllium foils prepared by vacuum evaporation were used as targets. Typical thicknesses were about 0.18 mg/cm², representing approximately 1-Mev energy loss for the incident nitrogen beam.

Early in the course of this experiment it was found that the beryllium foils contained oxygen, and scattering from it competed seriously with the desired scattering. For example, at 20 deg laboratory angle the

* Operated for the U. S. Atomic Energy Commission by Union Carbide Corporation.

¹ H. L. Reynolds and A. Zucker, Phys. Rev. **102**, 1378 (1956).

² E. Goldberg and H. L. Reynolds, Phys. Rev. **112**, 1981 (1959).

³ J. S. Blair, Phys. Rev. **95**, 1218 (1954).

⁴ Wegener, Eisberg, and Igo, Phys. Rev. **99**, 825 (1955).

⁵ Halbert, Handley, Pinajian, Webb, and Zucker, Phys. Rev. **106**, 251 (1957).